TÜBİTAK

Turk J Phys
33 (2009) , 69 – 80.

doi:10.3906/fiz-0806-5

Production of YBCO Superconductor Sample by Powder-In-Tube Method (PITM); and Effect of Cd and Ga Doping on the System

Serkan ALAGÖZ
İnönü University, Department of Physics, Malatya-TURKEY
e-mail: sealagoz@inonu.edu.tr

Received 30.06.2008

Abstract

In this study, $YBa_2Cu_3O_{7-\delta}$ and $Y_{0.5}X_{0.5}Ba_2Cu_3O_{7-\delta}$ (x = Ga, Cd) compounds are produced by Powder-In-Tube Method and electrical and physical characteristics of those samples were investigated. Following 3, 5 and 9 tons pressure applied to three sample groups ($YBa_2Cu_3O_{7-\delta}$, $Y_{0.5}Cd_{0.5}Ba_2Cu_3O_{7-\delta}$, $Y_{0.5}Ga_{0.5}Ba_2Cu_3O_{7-\delta}$), samples were examined via X-Ray diffraction, resistivity and SEM measurement. Considerable changes in Crystallographic properties of the YBCO samples, produced by using Powder-In-Tube Method for different pressure values, were observed. Under different magnetic fields conditions, resistance of the YBCO samples was measured and it was seen that samples had very pure and homogenous structure. Ga doping into YBCO composition had negative effect on superconducting phases. Cd doping of YBCO induced a more positive effect on the system than Ga doping. Contrary, Cd doping negatively affected electrical properties of the YBCO system.

Key Words: Superconducting composites, YBCO composition, Powder-In-Tube method, Cd and Ga doping.

1. Introduction

After discovery of High Temperature Superconductors (HTS) in 1986, much research have been done on a variety of superconductor systems and production methods to develop superconductors. In particular, a variety of methods were developed to increase current densities in HTS superconductors. One method is the Powder-In-Tube Method, or PITM, which provides advantage in production of, for example, superconductor cables, tapes, thin cable, and thick films. Researchers observed that sample production via PIT method improved superconducting properties. Sheathed superconducting tapes, cables and wires of YBCO materials were mostly fabricated by powder-in-tube (PIT) method and promising results were obtained for large-scale applications

[1–7]. Main advantage of this method is to enable development of such sample that are able to carry high critical current density and able to remove defects caused from sheathing.

One of the more remarkable developments in HTS comes from the development of (Bi, Pb)-2223 phase produced by PIT [8, 9], in which (Bi,Pb)-2223 was developed and observed carrying high current, which made it suitable for use in commercial applications. Critical current density J_c for the best cable sample produced as long as 100 m reached 1.7×10^8 $\mathrm{A\cdot m^{-2}}$ and it has feature of folding and rolling [10]. Y-123 thin film samples exhibit critical current densities J_c of about 1.3×10^8 $\mathrm{A\cdot m^{-2}}$ at 77 Kelvin temperature [11].

2. Experimental Details

2.1. Production method

In this study, samples were prepared by Solid State Reaction Method. $\mathrm{Y_2O_3}$, CuO, $\mathrm{Ga_2O_3}$, $\mathrm{Cd_2O_3}$ powders of 99.99% purity, and $\mathrm{BaCO_3}$ powder of 99% purity, combined in stoichiometric ratios, were used in production of samples. These powders were mixed for an hour in order to obtain homogenous mixtures.

In the first phase of research, superconductor samples of $\mathrm{YBa_2Cu_3O_{7-\delta}}$ were produced. The raw mixture was calcinated for 18 hours at 970 °C temperature. In the calcination process, oxygen gas was supplied to the powder samples at 500 °C temperature. After the first calcination, samples were removed from stove then crushed to a finer powder. Samples were then recalcinated under the same conditions as the first calcination. On completion of the second calcination, samples were reground and placed into 3 enclosed silver tubes, each of 30 mm length, 5 mm diameter. 3, 5 and 9 tons pressure were applied on silver tubes and these silver tubes were annealed in oxygen atmosphere, according to the profile shown in Figure 1.

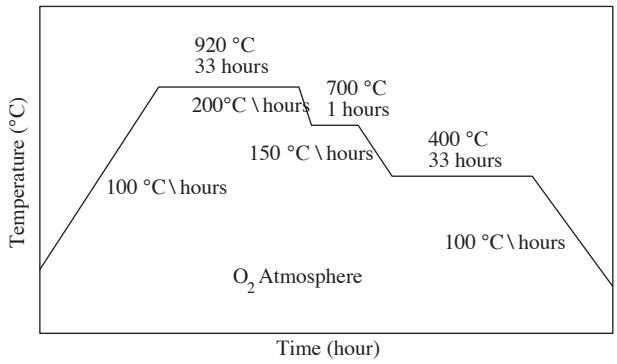

Figure 1. Annealing temperature profile of samples.

In the second phase, Gallium (Ga) and Cadmium (Cd) were stoichiometrically replaced with Yitrium doping. Compositions of $\mathrm{Y_{1-x}Cd_xBa_2Cu_3O_{7-\delta}}$, and $\mathrm{Y_{1-x}Ga_xBa_2Cu_3O_{7-\delta}}$ ($x = 0.5$) were obtained by doping Cd and Ga sources. Samples were then calcined and annealed in way similar to the treatment of $\mathrm{YBa_2Cu_3O_{7-\delta}}$ samples in Phase I. The thermal processes for all samples were done by using Carbolite TC 100 tube heater.

In Table 1 and Figure 1 are pressures and heat treatment temperature and duration applied to the samples studied. All samples seen in Table 1 were heat treated in oxygen atmosphere.

Table 1. Pressure, thermal process temperature and process time applied to samples.

Samples	Pressure (Ton)	Thermal process temperatures (°C)	Thermal process time
$YBa_2Cu_3O_{7-\delta}$	3	920	33 hours
$YBa_2Cu_3O_{7-\delta}$	5	920	33 hours
$YBa_2Cu_3O_{7-\delta}$	9	920	33 hours
$Y_{0.5}Ga_{0.5}Ba_2Cu_3O_{7-\delta}$	3	920	33 hours
$Y_{0.5}Ga_{0.5}Ba_2Cu_3O_{7-\delta}$	5	920	33 hours
$Y_{0.5}Ga_{0.5}Ba_2Cu_3O_{7-\delta}$	9	920	33 hours
$Y_{0.5}Cd_{\ 0.5}Ba_2Cu_3O_{7-\delta}$	3	920	33 hours
$Y_{0.5}Cd_{\ 0.5}Ba_2Cu_3O_{7-\delta}$	5	920	33 hours
$Y_{0.5}Cd_{\ 0.5}Ba_2Cu_3O_{7-\delta}$	9	920	33 hours

Resistance measurements of $YBa_2Cu_3O_{7-\delta}$ samples were done by using Cryogenic Q-3398 vibrating sample magnetometer with conventional four-probe method, at 10–120 K under 0, 3, 5 and 7 Tesla magnetic fields. Resistance measurements of Ga- and Cd-doped samples were done by a LakeShore 7000 series Susceptometer/Magnetometer system without magnetic field.

Crystal structure of the samples produced by using PIT method were examined via a Rigaku Rad-B x-ray diffractometer (XRD) system (using Cuk_α radiation $\lambda = 1.54056$ Å), which can do continuous and discontinuous measurements with 0.001° sensitivity between $2\theta = 1$–170° diffraction pattern. The XRD were scanned at 6°/min.

A Leo 430 scanning electron microscope was used to characterize the film surfaces. SEM images were captured with $\times 1500$ magnification.

3. Results and Discussion

3.1. X-ray diffraction results

X-Ray diffraction results for the $YBa_2Cu_3O_{7-\delta}$ sample produced via PIT method at 3, 5 and 9 tons pressure are illustrated in Figure 2. Calculated lattice parameters a, b and c are given in Table 2. (h, k, l) values calculated from unit cell parameters shows that samples has c-axis orientation and their structure has orthorhombic symmetry.

Table 2. a, b, c lattice parameters of $YBa_2Cu_3O_{7-\delta}$ samples produced under 3, 5 and 9 tons pressure.

Pressure	a(A)	b(A)	c(A)	d(A)
3 Ton	3.821	3.888	11.693	Orthorhombic
5 Ton	3.821	3.888	11.693	Orthorhombic
9 Ton	3.821	3.888	11.693	Orthorhombic

In the X-ray diffraction shown in Figure 2, distinguishable and strong characteristic $YBa_2Cu_3O_{7-\delta}$ peaks reveal purity of produced samples.

X-ray diffraction results for the $Y_{1-x}Cd_xBa_2Cu_3O_{7-\delta}$ ($x = 0.5$) samples produced by using PIT method at 3, 5 and 9 tons pressure are illustrated in Figure 3. In this figure, rise in impurity phases can be seen for the Cd-doped system. Peaks that belong to different phases ($Y_{0.5}Cd_{0.1}Ba_{3.6}O_x$, $Ba_{3.6}Cd_{1.2}Cu_5O_x$ and $Ba_{3.9}Cd_{1.4}Cu_{4.7}O_x$) were observed. But, any considerable changes in amplitude of the peaks are not seen in the figure. Cd doping drives $YBa_2Cu_3O_{7-\delta}$ structure into multi-phase system and reduces superconductivity. On the other hand, isostatic pressure applied to system does not have considerable effect on the system.

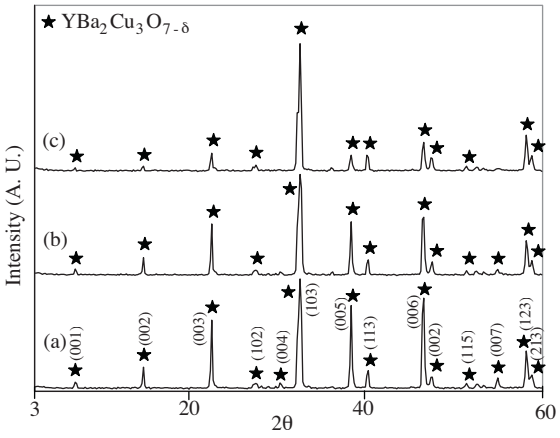

Figure 2. XRD patterns for $YBa_2Cu_3O_{7-\delta}$ samples produced under (a) 3 tons pressure, (b) 5 tons pressure and (c) 9 tons pressure.

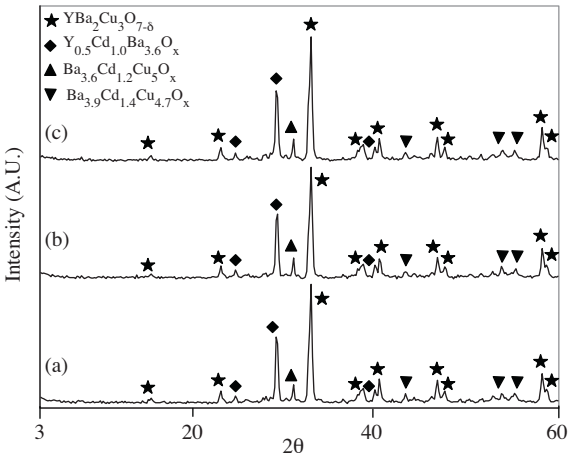

Figure 3. XRD patterns for $Y_{0.5}Cd_XBa_2Cu_3O_{7-\delta}$ (x=0.5) samples produced under (a) 3 tons pressure, (b) 5 tons pressure and (c) 9 tons pressure.

X-ray diffraction results for the $Y_{1-x}Ga_xBa_2Cu_3O_{7-\delta}$ ($x = 0.5$) samples produced by using PIT method at 3, 5 and 9 tons pressure are illustrated in Figure 4. Ga doping into the system decreases number and amplitude of characteristic $YBa_2Cu_3O_{7-\delta}$ peaks and drives the structure to multi-phase system. These impurity phases emerged in structure were seen to give rise negative effects on Ga superconductor phase. Applied isostatic pressure above 5 tons was observed to have positive effect on the system.

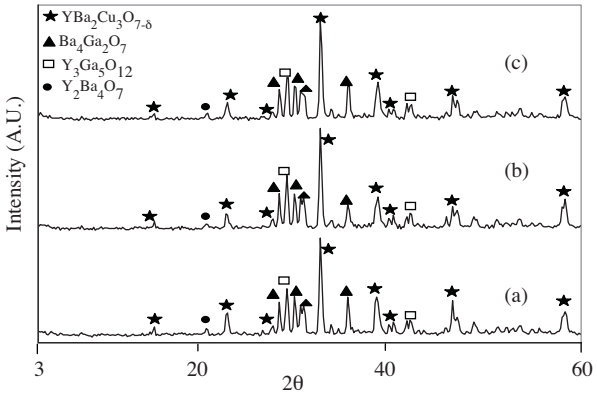

Figure 4. XRD patterns for $Y_{1-X}Ga_XBa_2Cu_3O_{7-\delta}$ (x=0.5) samples produced under (a) 3 tons pressure, (b) 5 tons pressure and (c) 9 tons pressure.

3.2. Resistivity measurement results

Resistivity measurements of the $YBa_2Cu_3O_{7-\delta}$ samples produced by using Powder-In-Tube method were done under magnetic fields of 0, 3, 5 and 7 Teslas. The Resistance-Temperature (R-T) curve for $YBa_2Cu_3O_{7-\delta}$ samples produced by using PIT Method with 3 tons pressure is shown in Figure 5. As the magnetic field applied on the sample increases, visible decreases in T_c and $T_c(0)$ temperature values were observed. Samples exhibits maximum T_c and $T_c(0)$ temperature when the magnetic field is completely removed from the volumes of the samples as a result of the Meissner effect. But, constantly raising the applied magnetic field leads to defects in the superconductor structure and reducing temperaturesT_c and $T_c(0)$. T_c and $T_c(0)$ as a function of applied magnetic field is shown in Table 3.

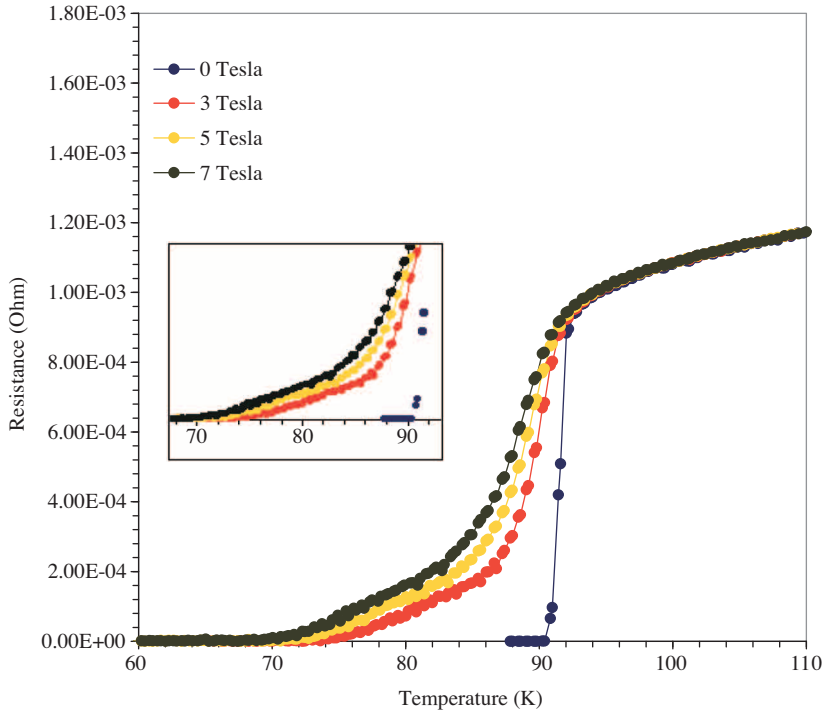

Figure 5. Resistance-Temperature curves versus magnetic field for $YBa_2Cu_3O_{7-\delta}$ sample produced by using PIT Method under 3 tons pressure.

Table 3. T_c and $T_c(0)$ temperature values respect to applied magnetic fields on $YBa_2Cu_3O_{7-\delta}$ sample produced by using PIT method under 3 tons pressure.

Applied Magnetic Field	T_c	$T_c(0)$
0 Tesla	93 K	91 K
3 Tesla	94 K	73 K
5 Tesla	93 K	70 K
7 Tesla	92 K	67 K

Resistance-Temperature curve for $YBa_2Cu_3O_{7-\delta}$ samples produced by using PIT method with 5 tons pressure is shown in Figure 6. Temperatures T_c and $T_c(0)$ versus applied magnetic field are given in Table 4. Note the rise in $T_c(0)$ temperature values compared to $T_c(0)$ temperature values in samples produced with 3 tons pressure. This may be because the added pressure gave rise to a more regular order in the grain structure.

Table 4. T_c and $T_c(0)$ temperature values respect to applied magnetic fields on $YBa_2Cu_3O_{7-\delta}$ sample produced by using PIT Method under 5 tons pressure.

Applied Magnetic Field	T_c	$T_c(0)$
0 Tesla	93 K	88 K
3 Tesla	92 K	78 K
5 Tesla	91 K	75 K
7 Tesla	91 K	74 K

Resistance-Temperature curve for $YBa_2Cu_3O_{7-\delta}$ samples produced by using PIT Method with 9 tons pressure is shown in Figure 7. T_c and $T_c(0)$ temperature values as a function of applied magnetic field are given in Table 5. With the applied pressure increased to 9 tons, there is a slight increase in T_c temperature value and a visible rise in $T_c(0)$, compared to samples produced under 5 tons pressure. This arises from the grain structure becoming closer packed and more ordered, forming a more aligned micro structure; thus the magnetic field exhibits less penetration into the structure.

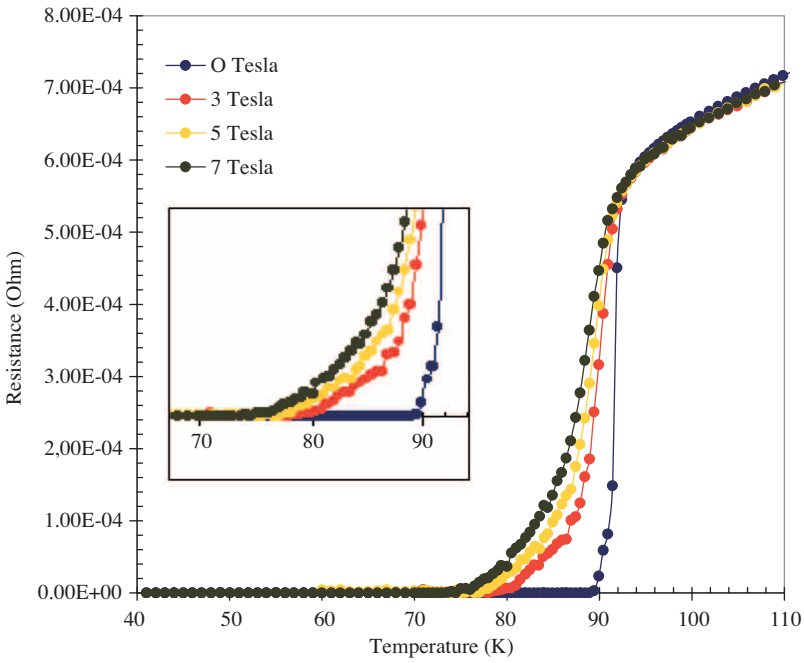

Figure 6. Resistance-Temperature curves versus magnetic field for $YBa_2Cu_3O_{7-\delta}$ sample produced by using PIT method under 5 tons pressure.

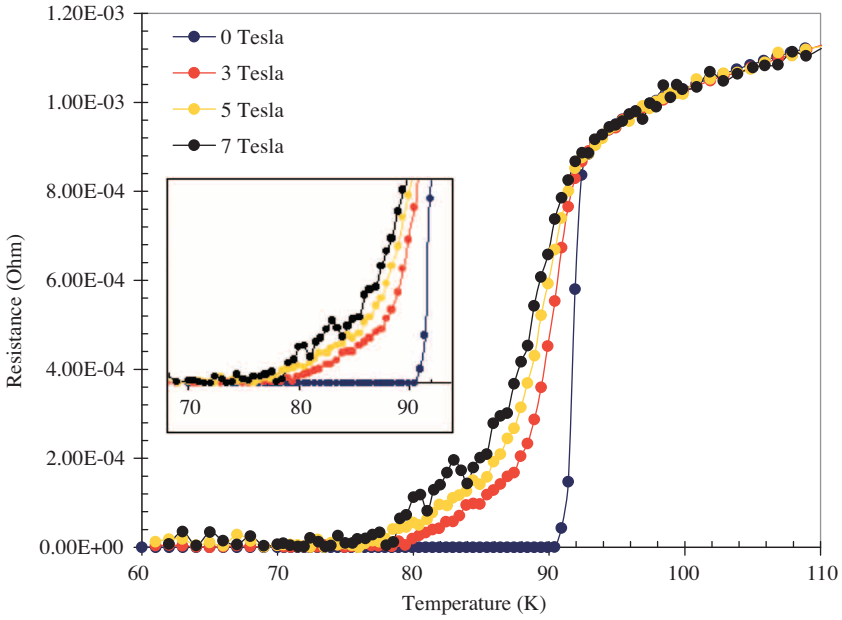

Figure 7. Resistance-Temperature curves versus magnetic field for $YBa_2Cu_3O_{7-\delta}$ sample produced by using PIT method under 9 tons pressure.

Table 5. T_c and $T_c(0)$ temperature values respect to applied magnetic fields on $YBa_2Cu_3O_{7-\delta}$ sample produced by using PIT method under 9 tons pressure.

Applied Magnetic Field	T_c	$T_c(0)$
0 Tesla	93 K	90 K
3 Tesla	92 K	79 K
5 Tesla	92 K	76 K
7 Tesla	92 K	76 K

Resistance-Temperature curves for Cd-doped $Y_{0.5}Cd_{0.5}Ba_2Cu_3O_{7-\delta}$ system produced by using PIT method with 3, 5 and 9 tons pressure are shown in Figure 8. T_c and $T_c(0)$ temperature values of Cd-doped samples versus applied pressure are given in Table 6. Decrease in T_c temperature is the result of moving the system from a single phase to a multi-phase system arising from Cd doping. Doping causes impurity phases to emerge, affecting the electronic order of Cu-O layers and also disturbs crystal structure coordination, since Cd-Y ionic diameters are different from each other. All these reasons act to change T_c. It was observed that increasing the pressure applied to Cd-doped samples did not change much T_c. Although applying more pressure to samples makes their structures better aligned, the increase in distances between atoms as result of Cd doping has a much more dominant effect on the micro structure of the system. Resistance-Temperature plots shown in Figure 8 show that all samples have superconducting properties and transition temperatures T_c around 85–90 Kelvin.

Table 6. T_c and $T_c(0)$ temperature values for $Y_{0.5}Cd_{0.5}Ba_2Cu_3O_{7-\delta}$ sample produced by using PIT method under 3, 5 and 9 tons pressure.

Applied Pressure	T_c	$T_c(0)$
3 Ton	90 K	78 K
5 Ton	88 K	80 K
9 Ton	85 K	78 K

Resistance-Temperature curves for Ga-doped $Y_{0.5}Ga_{0.5}Ba_2Cu_3O_{7-\delta}$ system produced by using PIT method with 3, 5 and 9 tons pressure are shown in Figure 9. As one can see in the figure, Ga doping and increasing pressure leads to the complete disappearance of the superconducting state. The crystal structure is disturbed since the ionic diameter of Ga^{+3} (0.62 Å) is smaller than the ionic diameter of Y^{+3} (1.02 Å), hence disturbance in the electronic configuration of the system. Difference between ionic diameters also leads to increasing distance between atoms. In this case, oxygen concentration between layers (Cu-O) varies resulting inloss of the superconducting state.

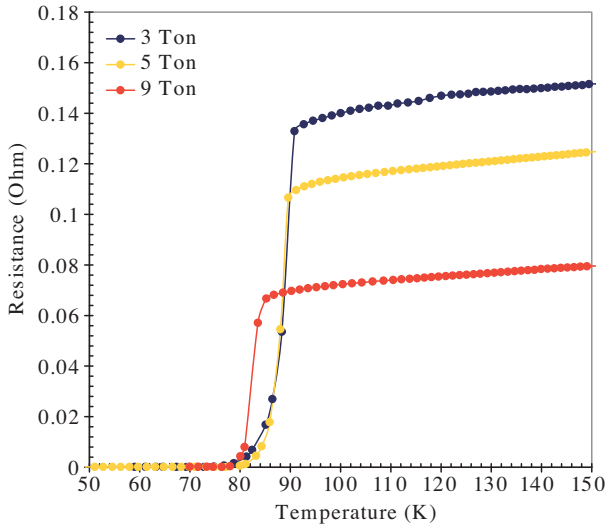

Figure 8. Resistance-Temperature curves for $Y_{0.5}Cd_{0.5}Ba_2Cu_3O_{7-\delta}$ sample produced by using PIT method under 3, 5 and 9 tons pressure.

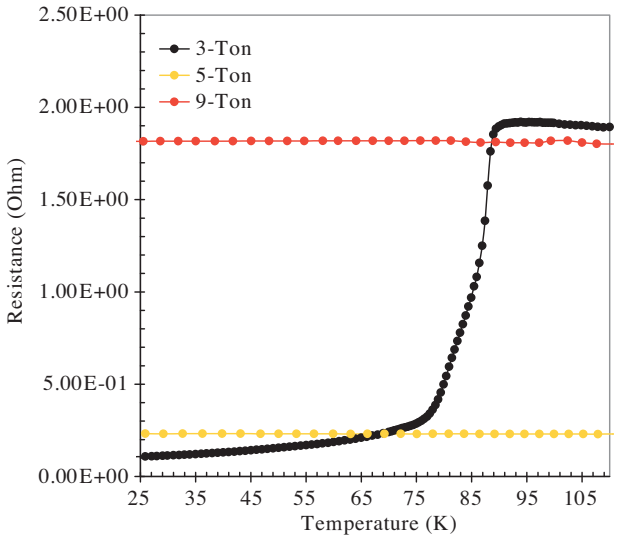

Figure 9. Resistance-Temperature curves for $Y_{0.5}Ga_{0.5}Ba_2Cu_3O_{7-\delta}$ sample produced by using PIT method under 3, 5 and 9 tons pressure.

Comparing the electronic configuration of Ga $(\ldots 3d^{10}\ 4s^2\ 4p^1)$ to that of Yttrium $(\ldots 4d^1\ 5s^2)$, one can see Ga is more likely than Yttrium to bond with oxygen in $Y_{0.5}Ga_{0.5}Ba_2Cu_3O_{7-\delta}$ hence cause oxygen reduction in the Cu-O layer.

Figure 9 shows that Ga-doped samples do not have superconducting properties. Although, Ga doped sample produced under 3 tons pressure has a transition temperature at 89 Kelvin, it does not have a zero resistance temperature. The resistance of Ga-doped samples produced under 5 and 9 tons pressure exhibited very little variation during the whole cooling process.

3.3. SEM results

SEM images of YBCO samples produced by PIT method under 3, 5 and 9 tons pressure are shown in Figures 10(a), (b) and (c). Granular structure of classical YBCO composition is clearly seen in Figure 10(a) for the sample produced under 3 tons pressure. Classical structuring, with grain size varying 2–15 mm, was explicitly seen. Space between grains, which was result of low pressure, was also seen in Figure 10.

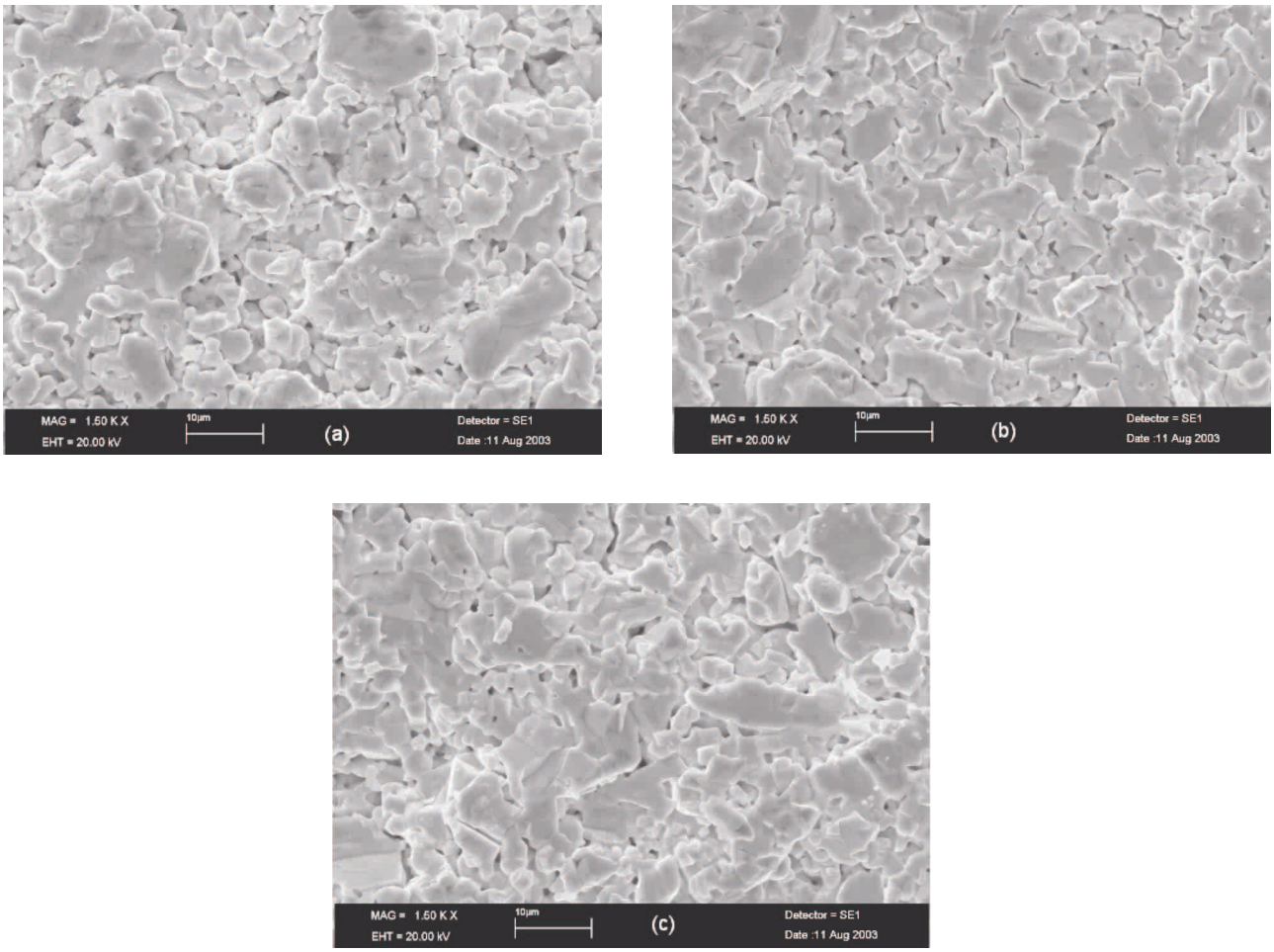

Figure 10. SEM images of YBCO samples produced under (a) 3 tons pressure, (b) 5 tons pressure and (c) 9 tons pressure.

SEM images of $Y_{0.5}Cd_{0.5}Ba_2Cu_3O_{7-\delta}$ samples produced by PIT method under 3, 5 and 9 tons pressure are shown in Figures 11(a), (b) and (c). Considering and comparing with images 10(a)–(c), one can see an apparent change in surface formation on $Y_{0.5}Cd_{0.5}Ba_2Cu_3O_{7-\delta}$ samples. For example, in Figure 11(a), zone of partial melting in the sample produced under 3 tons pressure is larger than that for YBCO system; yet, very large spaces between roughly 10–20 mm sized half melting crystal region are observed in the image and, as discussed earlier, would effect the structure's electrical properties. In Figure 11(b), melting zones resulting from increasing pressure are more visible and space between grains were of similar size. These situation is more clearly seen in the image of the sample produced under 9 tons pressure, shown in Figure 11(c).

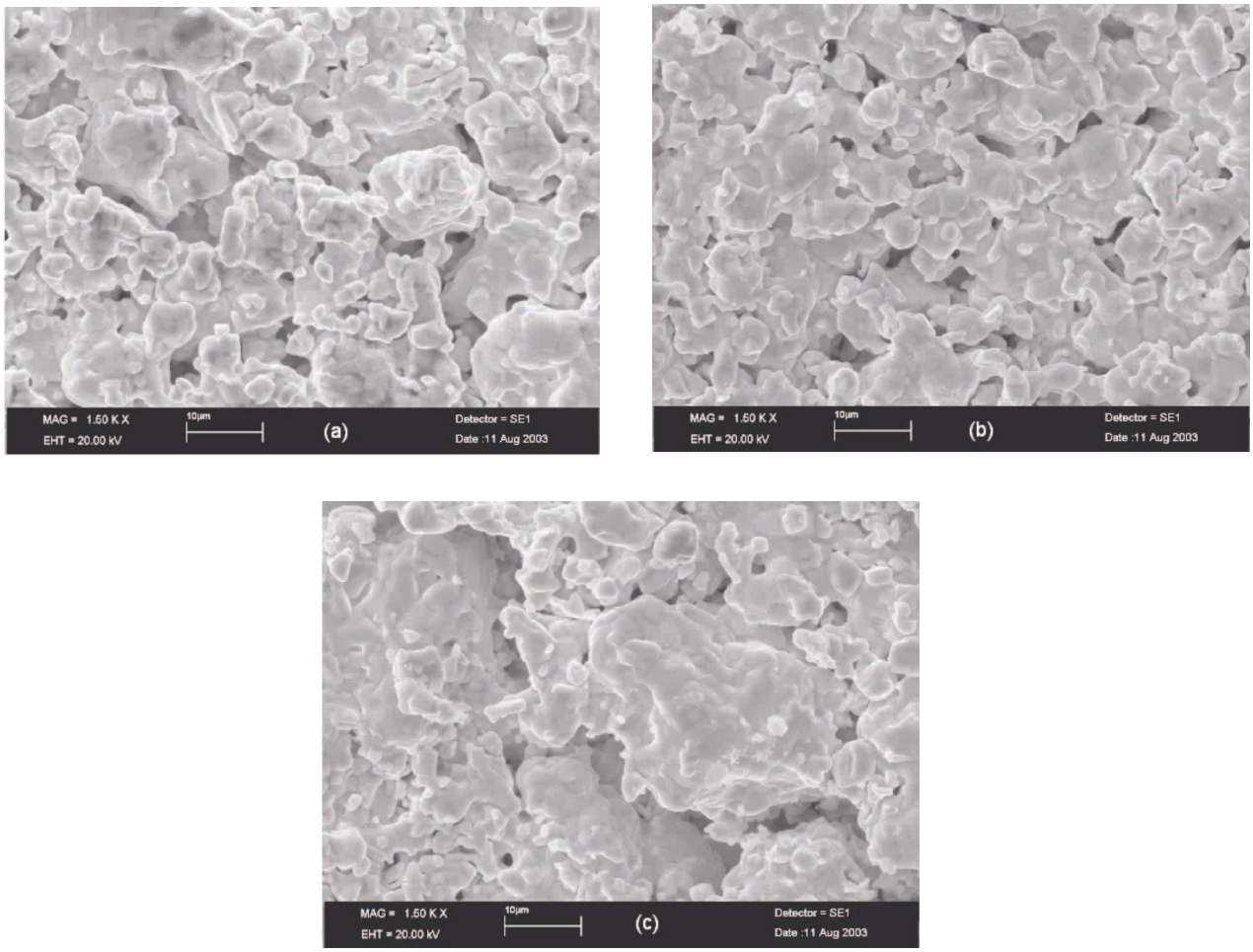

Figure 11. SEM images of Cd doping samples produced under (a) 3 tons pressure, (b) 5 tons pressure and (c) 9 tons pressure.

As a result of the present work, we see that grains of roughly the same size, of non-uniform shape and not having undergone partial melting are undesirable characteristics as they predict the loss of losing superconducting properties. Such structuring is often seen in Ga-doped samples.

In the Figures 12(a), (b) and (c), SEM images of $Y_{0.5}Ga_{0.5}Ba_2Cu_3O_{7-\delta}$ samples produced by PIT method under 3, 5 and 9 tons pressure are shown.

4. Conclusion

In our study, YBCO samples were successfully produced by using PIT method. Results obtained from XRD and SEM showed that structure of samples was highly pure and homogenous. Cd- and Ga-doped YBCO system leads to multi-phase structuring. Ga doping together with increased pressure led to loss of the superconducting state.

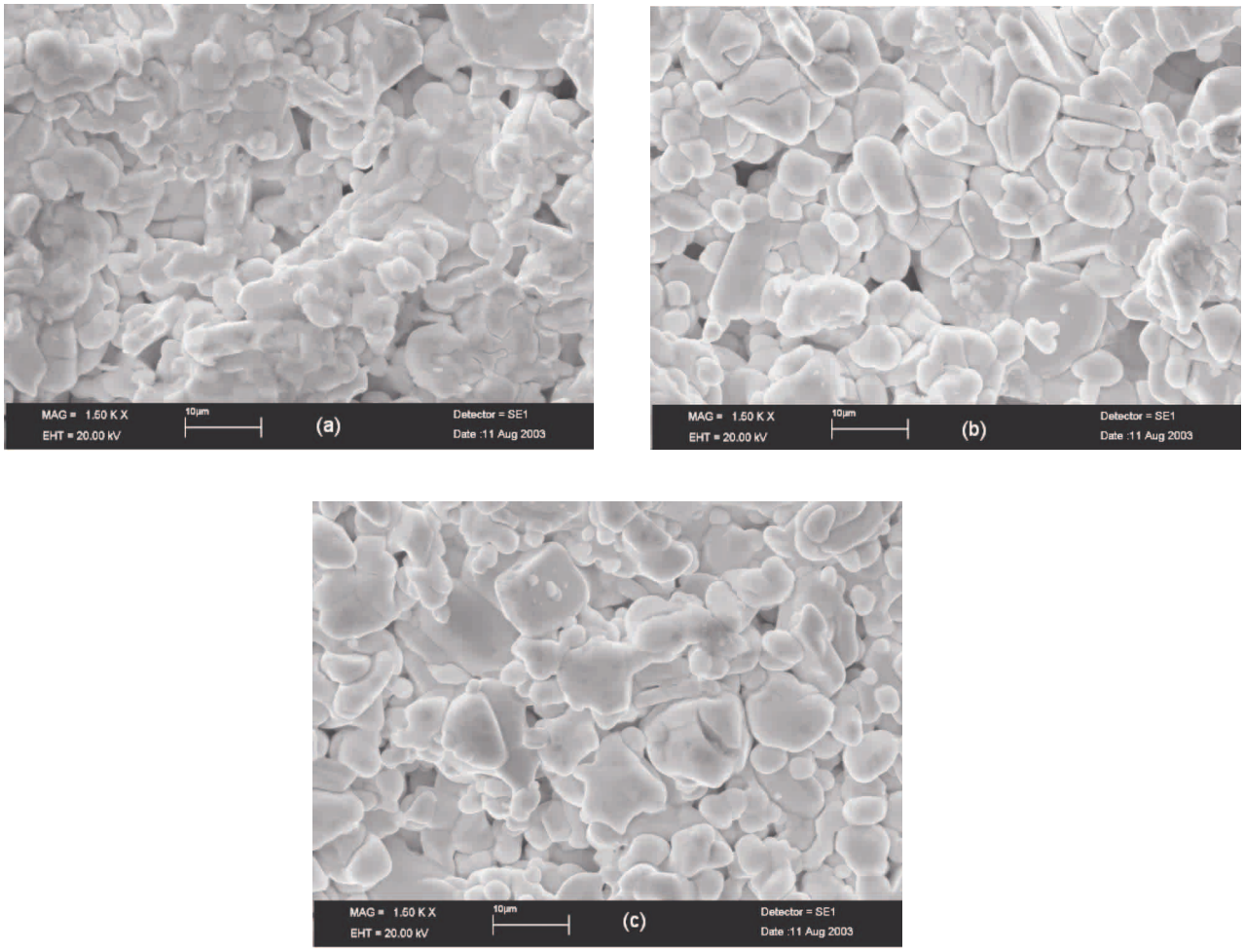

Figure 12. SEM images of Ga doping samples produced under (a) 3 tons pressure, (b) 5 tons pressure and (c) 9 tons pressure.

We observed that increasing production pressure of $YBa_2Cu_3O_{7-\delta}$ led to rising $T_c(0)$ temperature under variety magnetic fields (see Table 3, 4, 5) by narrowing gaps in the $YBa_2Cu_3O_{7-\delta}$ structure. These narrowed gaps reduced magnetic field pennetration into the superconductor volume.

References

[1] Z. Han, P. Skov-Hansen, T. Freltoft, *Supercond. Sci. Technol.*, **10**, (1997), 371.

[2] P. Paturi, J. Raittila, J. C. Grivel, H. Huhtinen, B. Seifi, R. Laiho, N. H. Andersen, *Physica C*, **372-376**, (2002), 779.

[3] P. Paturi, T. Kulmala, J. Raittila, J.-C. Grivel, R. Laiho, N. H. Andersen, *Physica C*, **408-410**, (2004), 935.

[4] B. Glowacki, *Supercond. Sci. Technol.*, **11**, (1998), 989.

[5] E. Blinov, V. G. Fleisher, H. Huhtinen, R. Laiho, E. Lähderanta, P. Paturi, Yu. P. Stepanov, L. Vlasenko, *Supercond. Sci. Technol.*, **10**, (1997), 818.

[6] N. M. Alford, S. J. Penn , T. W. Button, *Supercond. Sci. Technol.*, **10**, (1997), 169.

[7] R. Zeng, H. K. Lui, S. X. Dou, *Physica C*, **300**, (1998), 49.

[8] J. Tenbrink, M. Wilhelm, K. Heine, H. Krauth, *IEEE Trans. Magn.*, **27**, (1991),1239.

[9] D. C. Larbalestier, X. Y. Cai, Y. Feng, H. Edelman, A. Umezawa, G. N. Riley, Jr and W. L. Carter, *Physica C*, **221**, (1994), 299.

[10] M. J. Minot, W. L. Carter, J. J. Jr Gannon, R. S. Hamilton, P. K. Miles, D. R. Parker, G. N. Jr Riley, M. Rupich, M. R. Teplitsky, E. D. Thompson, K. Zafar, J., *Mater. Chem.*, **7**, (1997), 653.

[11] S.R. Foltyn, *Proc. MRS Spring Meeting*, (1995).